Inorg. Chem. **2007**, *46*, 6427–6436

Anion-Selective Interaction and Colorimeter by an Optical Metalloreceptor Based on Ruthenium(II) 2,2′-Biimidazole: Hydrogen Bonding and Proton Transfer

Ying Cui, Hao-Jun Mo, Jin-Can Chen, Yan-Li Niu, Yong-Rui Zhong, Kang-Cheng Zheng, and Bao-Hui Ye*

MOE Laboratory of Bioinorganic and Synthetic Chemistry, School of Chemistry and Chemical Engineering, Sun Yat-Sen University, Guangzhou 510275, China

Received March 8, 2007

A new anion sensor $[Ru(bpy)_2(H_2biim)](PF_6)_2$ (**1**) (bpy = 2,2′-bipyridine and H_2biim = 2,2′-biimidazole) has been developed, in which the Ru(II)-bpy moiety acts as a chromophore and the H_2biim ligand as an anion receptor via hydrogen bonding. A systematic investigation shows that **1** is an eligible sensor for various anions. It donates protons for hydrogen bonding to Cl^-, Br^-, I^-, NO_3^-, HSO_4^-, $H_2PO_4^-$, and OAc^- anions and further actualizes monoproton transfer to the OAc^- anion, changing color from yellow to orange brown. The fluoride ion has a high affinity toward the N–H group of the H_2biim ligand for proton transfer, rather than hydrogen bonding, because of the formation of the highly stable HF_2^- anion, resulting in stepwise deprotonation of the two N–H fragments. These processes are signaled by vivid color changes from yellow to orange brown and then to violet because of second-sphere donor–acceptor interactions between Ru(II)-H_2biim and the anions. The significant color changes can be distinguished visually. The processes are not only determined by the basicity of anion but also by the strength of hydrogen bonding and the stability of the anion–receptor complexes. The design strategy and remarkable photophysical properties of sensor **1** help to extend the development of anion sensors.

Introduction

Anion-selected recognition and sensing is of great interest because anions are known to play numerous fundamental roles in chemical, biological, and environmental processes.[1−5] A convenient and efficient strategy to design a colorimetric anion sensor is to combine an anion receptor with a chromogenic moiety, which shows a color change that is visible to the naked eye when the binding event takes place. Generally, the chromophores may be organic compounds or metal−organic complexes, and binding sites with hydrogen-bonding donors or receptors containing urea,[1d,6] thiourea,[7] amide,[8] phenol,[9] imidazole ion,[10] or pyrrole[11] subunits have been well exploited. Because of their excellent redox and photo properties, particularly, absorption and emission spectra within the visible range, Ru(II) polypyridyl complexes have

* To whom correspondence should be addressed. Fax: (86)-20-84112245. Phone: (86)-20-84112469. E-mail: cesybh@mail. sysu.edu.cn.

(1) (a) Beer, P. D.; Gale, P. A. *Angew. Chem., Int. Ed.* **2001**, *40*, 486. (b) Sessler, J. L.; Davis, J. M. *Acc. Chem. Res.* **2001**, *34*, 989. (c) Martinez-Manez, R.; Sancenon, F. *Chem. Rev.* **2003**, *103*, 4419. (d) Amendola, V.; Gómez, E. D.; Fabbrizzi, L.; Licchelli, M. *Acc. Chem. Res.* **2006**, *39*, 343. (e) Bowman-James, K. *Acc. Chem. Res.* **2005**, *38*, 671.

(2) Gale, P. A., Ed. 35 Years of Synthetic Anion Receptor Chemistry 1968−2003. *Coord. Chem. Rev.* **2003**, *240*, 1−226.

(3) *Anion Sensing*; Stibor, I., Ed.; Topics in Current Chemistry 255; Springer-Verlag: Berlin, 2005.

(4) *Anion Receptor Chemistry;* Sessler, J. L., Gale, P. A., Cho, W. S., Stoddart, J. F., Eds.; Monographs in Supramolecular Chemistry; Royal Society of Chemistry: Cambridge, U.K.; 2006.

(5) Gale, P. A., Ed. Anion Coordination Chemistry II. *Coord. Chem. Rev.* **2006**, *250*, 2917−3244.

(6) (a) Cho, E. J.; Moon, J. W.; Ko, S. W.; Lee, J. Y.; Kim, S. K.; Yoon, J.; Nam, K. C. *J. Am. Chem. Soc.* **2003**, *125*, 12376. (b) Descalzo, A. B.; Rurack, K.; Weisshoff, H.; Martinez-Manez, R.; Marcos, M. D.; Amoros, P.; Hoffmann, K.; Soto, J. *J. Am. Chem. Soc.* **2005**, *127*, 184. (c) Hay, B. P.; Firman, T. K.; Moyer, B. A. *J. Am. Chem. Soc.* **2005**, *127*, 1810. (d) Otón, F.; Tárraga, A.; Espinosa, A.; Velasco, M. D.; Molina, P. *J. Org. Chem.* **2006**, *71*, 4590. (e) Wu, Y.; Peng, X.; Fan, J.; Gao, S.; Tian, M.; Zhao, J.; Sun, S. *J. Org. Chem.* **2007**, *72*, 62.

(7) (a) Jose, D. A.; Kumar, D. K.; Ganguly, B.; Das, A. *Org. Lett.* **2004**, *6*, 3445. (b) Gunnlaugsson, T.; Kruger, P. E.; Jensen, P.; Tierney, J.; Ali, H. D. P.; Hussey, G. M. *J. Org. Chem.* **2005**, *70*, 10875. (c) Gómez, E. D.; Fabbrizzi, L.; Licchelli, M.; Monzani, E. *Org. Biomol. Chem.* **2005**, *3*, 1495. (d) Pfeffer, F. M.; Gunnlaugsson, T.; Jensen, P.; Kruger, P. E. *Org. Lett.* **2005**, *7*, 5357. (e) Thiagarajan, V.; Ramamurthy, P.; Thirumalai, D.; Ramakrishnan, V. T. *Org. Lett.* **2005**, *7*, 657. (f) Amendola, V.; Gómez, E. D.; Fabbrizzi, L.; Licchelli, M.; Monzani, E.; Sancenón, F. *Inorg. Chem.* **2005**, *44*, 8690. (g) Gunnlaugsson, T.; Glynn, M.; Tocci, G. M.; Kruger, P. E.; Pfeffer, F. M. *Coord. Chem. Rev.* **2006**, *250*, 3094.

10.1021/ic7004562 CCC: $37.00
Published on Web 06/30/2007

been widely employed as chromophores, in which functional groups such as various acyclic, macrocyclic, and calixarenes are appended and form hydrogen bonds with anions.[1a,1c,12,13] Many complexes containing 2,2′-bipyridine (bpy)[13−17] and 1,10-phenanthroline,[18−21] based on the chelating ligands, have been designed via the incorporation of different appended hydrogen-bonding donor groups for the construction of a variety of anion sensors. However, it is not easy to clearly distinguish between a hydrogen-bonding donor binding to an anion and a process in which the hydrogen-bonding donor is deprotonated and proton transferred to a basic anion.[22] Because these processes are complicated and may be controlled by several factors: (i) the acidity of metalloreceptor, (ii) the basicity of anion, and (iii) the strength and amount of hydrogen bonding, which may be highly related to the charge numbers and the shape of the match between the hydrogen-bonding donor and acceptor groups.

In our quest for appropriate ligands for the construction of colorimetric anion sensors and distinction between hydrogen bonding and proton transfer, we have found that an Ru(II)-bpy complex containing 2,2′-biimidazole (H_2biim) is a good candidate because it donates protons for hydrogen bonding to anions. While the Ru(II)-bpy moiety has characteristic absorption and emission spectra within the visible range and acts as a chromophore, the H_2biim ligand has a bifunctionality: the imino moieties can be coordinated to a Ru(II)-bpy fragment, and the amino groups may donate 2-fold hydrogen bonding to an anion. The most interesting and important features are the following: (i) this combination will improve solubility of the sensor (H_2biim sparingly dissolves in common solvents) and facilitate observation of the interaction with anions in solution; (ii) the chelating coordination model enforces the *syn* conformation and then engages in hydrogen bonding via the externally directed pair of N−H groups of the H_2biim ligand with a wide range of anions; (iii) the chelating coordination markedly increases the acidity of the metal-H_2biim complex ($pK_{a1} = 7.2$ and $pK_{a2} = 12$, whereas the pK_{a1} of free H_2biim is ∼11.5),[23] which provides a good example to observe proton transfer via the formation of hydrogen bonding or deprotonation in the presence of a more basic anion as an acceptor. Indeed, the H_2biim complexes have been found to extensively form hydrogen bonds with external anions, such as halide,[24] nitrate,[25] and carboxylate[26−29] in the solid state and to exhibit self-assembly via complementary hydrogen bonding in crystal engineering (where each H_2biim ligand is a monodeprotonated, anionic imidazole ring).[30,31] The bi-deprotonated species ($biim^{2-}$) has also been observed in strong basic conditions and assembled into polynuclear complexes.[32] However, a systematic insight into the solution behavior of the H_2biim complex as a receptor for various anions is quite rare.[33,34]

The Ru(II)-bpy complex containing H_2biim can interact with various anions via the formation of hydrogen bonding,

(8) (a) Camiolo, S.; Gale, P. A.; Hursthouse, M. B.; Light, M. E.; Warriner, C. N. *Tetrahedron Lett.* **2003**, *44*, 1367. (b) Kim, S. K.; Bok, J. H.; Bartsch, R. A.; Lee, J. Y.; Kim, J. S. *Org. Lett.* **2005**, *7*, 4839. (c) Gale, P. A. *Chem. Commun.* **2005**, 3761. (d) Kim, H. J.; Kim, S. K.; Lee, J. Y.; Kim, J. S. *J. Org. Chem.* **2006**, *71*, 6611. (e) Li, Y.; Cao, L.; Tian, H. *J. Org. Chem.* **2006**, *71*, 8279.

(9) (a) Lee, D. H.; Lee, K. H.; Hong, J. I. *Org. Lett.* **2001**, *3*, 5. (b) Lee, D. H.; Lee, H. Y.; Lee, K. H.; Hong, J. I. *Chem. Commun.* **2001**, 1188. (c) Zhang, X.; Guo, L.; Wu, F. Y.; Jiang, Y. B. *Org. Lett.* **2003**, *5*, 2667.

(10) Chellappan, K.; Singh, N. J.; Hwang, I. C.; Lee, J. W.; Kim, K. S. *Angew. Chem., Int. Ed.* **2005**, *44*, 2899.

(11) (a) Chang, K.-J.; Moon, D.; Lah, M. S.; Jeong, K.-S. *Angew. Chem., Int. Ed.* **2005**, *44*, 7926. (b) Nishiyabu, R.; Palacios, M. A.; Dehaen, W.; Anzenbacher, P. Jr. *J. Am. Chem. Soc.* **2006**, *128*, 11496.

(12) (a) de Silva, A. P.; Guarantne, H. Q.; Gunnlaugsson, N. T.; Huxley, A. J.; McCoy, C. P.; Rademacher, J. T.; Rice, T. R. *Chem. Rev.* **1997**, *97*, 1515. (b) Schubert, U. S.; Eschbaumer, C. *Angew. Chem., Int. Ed.* **2002**, *41*, 2893. (c) Browne, W. R.; Hage, R.; Vos, J. G. *Coord. Chem. Rev.* **2006**, *250*, 1653. (d) Medlycott, E. A.; Hanan, G. S. *Coord. Chem. Rev.* **2006**, *250*, 1763.

(13) (a) Beer, P. D. *Acc. Chem. Res.* **1998**, *31*, 71. (b) Beer, P. D.; Cadman, J. *Coord. Chem. Rev.* **2000**, *205*, 131. (c) Beer, P. D.; Hayes, E. J. *Coord. Chem. Rev.* **2003**, *240*, 167. (d) Beer, P. D.; Bayly, S. R. *Top. Curr. Chem.* **2005**, *255*, 125.

(14) (a) Szemes, F.; Hesek, D.; Chen, Z.; Dent, S. W.; Drew, M. G. B.; Goulden, A. J.; Graydon, A. R.; Grieve, A.; Mortimer, R. J.; Wear, T.; Weightman, J. S.; Beer, P. D. *Inorg. Chem.* **1996**, *35*, 5868. (b) Beer, P. D.; Szemes, F.; Balzani, V.; Sala, C. M.; Drew, M. G. B.; Dent, S. W.; Maestri, M. *J. Am. Chem. Soc.* **1997**, *119*, 11864. (c) Vickers, M. S.; Martindale, K. S.; Beer, P. D. *J. Mate. Chem.* **2005**, *15*, 2784.

(15) Watanabe, S.; Onogawa, O.; Komatsu, Y.; Yoshida, K. *J. Am. Chem. Soc.* **1998**, *120*, 229.

(16) Deetz, M. J.; Smith, B. D. *Tetrahedron Lett.* **1998**, *39*, 6841.

(17) Aoki, S.; Zulkefeli, M.; Shiro, M.; Kohsako, M.; Takeda, K.; Kimura, E. *J. Am. Chem. Soc.* **2005**, *127*, 9129.

(18) Anzenbacher, P., Jr.; Tyson, D. S.; Jursikova, K.; Castellano, F. N. *J. Am. Chem. Soc.* **2002**, *124*, 6232.

(19) Mizuno, T.; Wei, W.-H.; Eller, L. R.; Sessler, J. L. *J. Am. Chem. Soc.* **2002**, *124*, 1134.

(20) Lazarides, T.; Miller, T. A.; Jeffery, J. C.; Ronson, T. K.; Adams, H.; Ward, M. D. *Dalton Trans.* **2005**, 528.

(21) (a) Lin, Z.-H.; Ou, S.-J.; Duan, C.-Y.; Zhang, B.-G.; Bai, Z.-P. *Chem. Commun.* **2006**, 624. (b) Lin, Z.-H.; Zhao, Y.-G.; Duan, C.-Y.; Zhang, B.-G.; Bai, Z.-P. *Dalton Trans.* **2006**, 3678.

(22) Evans, L. S.; Gale, P. A.; Light, M. E.; Quesada, R. *Chem. Commun.* **2006**, 965.

(23) (a) Haga, M.-A. *Inorg. Chim. Acta.* **1983**, *75*, 29. (b) Rillema, D. P.; Sahai, R.; Matthews, P.; Edwards, A. K.; Shaver, R. J.; Morgan, L. *Inorg. Chem.* **1990**, *29*, 167. (c) Holmes, F.; Jones, K. M.; Torrible, E. G. *J. Chem.* Soc. **1961**, 4790.

(24) (a) Fortin, S.; Fabre, P.-L.; Dartiguenave, M.; Beauchamp, A. L. *J. Chem. Soc., Dalton Trans.* **2001**, 3520. (b) Atencio, R.; Ramırez, K.; Reyes, J. A.; Gonzalez, T.; Silva, P. *Inorg. Chim. Acta.* **2005**, *358*, 520.

(25) Maiboroda, A.; Rheinwald, G.; Lang, H. *Eur. J. Inorg. Chem.* **2001**, 2263.

(26) Martinez-Lorente, M. A.; Daham, F.; Sanakis, Y.; Petrouleas, V.; Bousseksou, A.; Tuchagues, J.-P. *Inorg. Chem.* **1995**, *34*, 5346.

(27) (a) Ye, B.-H.; Xue, F.; Xue, G.-Q.; Ji, L.-N. Mak, T. C. W. *Polyhedron* **1999**, *18*, 1785. (b) Ye, B.-H.; Ding, B.-B.; Weng, Y.-Q.; Chen, X.-M. *Inorg. Chem.* **2004**, *43*, 6866. (c) Ye, B.-H.; Ding, B.-B.; Weng, Y.-Q.; Chen, X.-M. *Cryst. Growth Des.* **2005**, *5*, 801. (d) Ding, B.-B.; Weng, Y.-Q.; Mao, Z.-W.; Lam, C.-K.; Chen, X.-M.; Ye, B.-H. *Inorg. Chem.* **2005**, *44*, 8836. (e) Ding, B.-B.; Weng, Y.-Q.; Cui, Y.; Chen, X.-M.; Ye, B.-H. *Supramol. Chem.* **2005**, *17*, 475.

(28) (a) Rau, S.; Böttcher, L.; Schebesta, S.; Stollenz, M.; Görls, H.; Walther, D. *Eur. J. Inorg. Chem.* **2002**, 2800. (b) Atencio, R.; Chacon, M.; Gonzalez, T.; Briceno, A.; Agrifoglio, G.; Sierraalta, A. *Dalton Trans.* **2004**, 505. (c) Larsson, K.; Öhrström, L. *CrystEngComm* **2004**, *6*, 354.

(29) (a) Tadokoro, M.; Fukui, S.; Kitajima, T.; Nagao, Y.; Ishimaru, S.; Kitagawa, H.; Isobe, K.; Nakasuji, K. *Chem. Commun.* **2006**, 1274. (b) Ghosh, A. K.; Jana, A. D.; Ghoshal, D.; Mostafa, G.; Chaudhuri, N. R. *Cryst. Growth Des.* **2006**, *6*, 701. (c) Sang, R.-L.; Xu, L. *Inorg. Chim. Acta.* **2006**, *359*, 525.

(30) (a) Tadokoro, M.; Nakasuji, K. *Coord. Chem. Rev.* **2000**, *98*, 205. (b) Tadokoro, M.; Kanno, H.; Kitajima, T.; Shimada-Umemoto, H.; Nakanishi, N.; Isobe, K.; Nakasuji, K. *Proc. Nat. Acad. Sci. U. S. A* **2002**, *99*, 4950.

(31) Öhrström, L.; Larsson, K. *Dalton Trans.* **2004**, 347.

Scheme 1. Schematic Representation of the Interaction between Sensor **1** and Anions

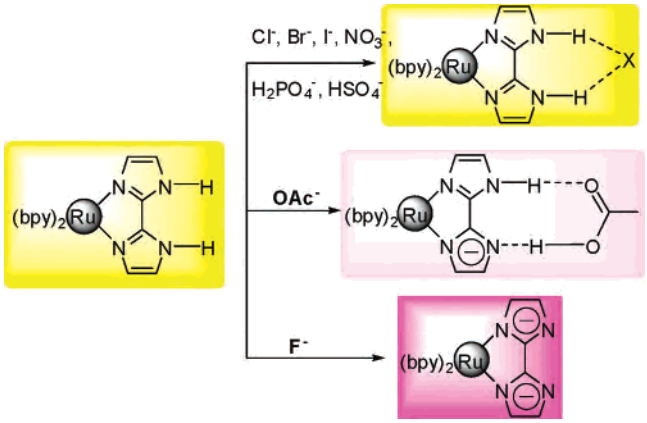

Table 1. Crystal Data and Structure Refinement for Complex **2**

molecular formula	$C_{26}H_{23}N_{11}ORu$
fw	606.62
cryst syst	monoclinic
space group	$P2_1/c$
a (Å)	12.1028(12)
b (Å)	19.068(2)
c (Å)	12.8736(13)
β (deg)	117.028(2)
V (Å^3)	2646.5(5)
Z	4
ρ_{calcd} (g cm^{-3})	1.523
μ (mm^{-1})	0.635
reflns collected	20 919
independent reflns	5782
data/restraints/params	3998/0/360
R1[a] [$I > 2\sigma(I)$],	0.0381,
wR2[b] (all data)	0.0694
$\Delta\rho_{max}/\Delta\rho_{min}$ (e Å^{-3})	0.89/−0.46

[a] $R1 = \sum||F_o| - |F_c||/\sum|F_o|$. [b] $wR2 = [\sum w(F_o^2 - F_c^2)^2/\sum w(F_o^2)^2]^{1/2}$.

and these processes can be distinguished visually because of the color changes that occur upon mono- and bi-deprotonation. We report herein a systematic insight into the interactions of $[Ru(bpy)_2(H_2biim)](PF_6)_2$ (**1**) with various anions such as Cl^-, Br^-, I^-, NO_3^-, HSO_4^-, $H_2PO_4^-$, OAc^-, and F^-. Because of the different basicities and hydrogen-bonding capabilities of the aforementioned anions, they can be distinguished by the different color outputs (Scheme 1).

Experimental Section

Materials and Methods. The reagents and solvents employed were commercially available and were used as received without further purification. The C, H, and N microanalyses were carried out with a Vario EL elemental analyzer. The FT-IR spectra were recorded from KBr pellets in the range of 400−4000 cm^{-1} on a Bruker-EQUINOX 55 FT-IR spectrometer. ^{1}H NMR spectra were recorded on a Varian Mercury-Plus 300 NMR spectrometer with chemical shifts (ppm) relative to tetramethylsilane (TMS). Electron spray ionization (ESI) mass spectra were obtained on a LCQ DECA XP quadrupole ion trap mass spectrometer with MeCN as the carrier solvent. *cis*-$[Ru(bpy)_2Cl_2]\cdot 2H_2O$ and $[Ru(bpy)_2(H_2biim)]Cl_2$ (**3**) were synthesized using literature procedures.[35,36]

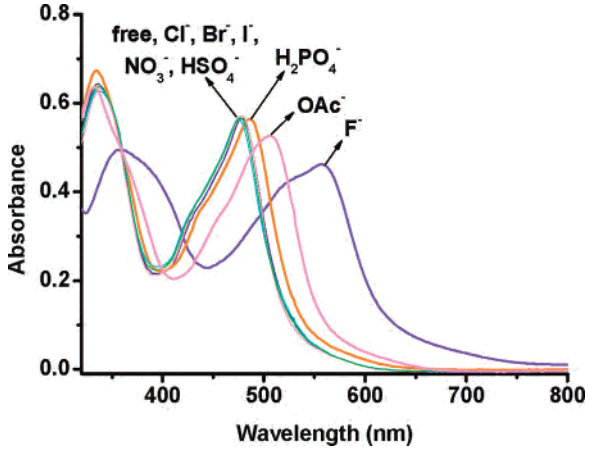

Figure 1. UV−vis spectra of **1** in MeCN solution (5×10^{-5} M, black) and the addition of 1 equiv of Cl^- (navy), Br^- (yellow), I^- (cyan), NO_3^- (green), HSO_4^- (blue), $H_2PO_4^-$ (organ), and OAc^- (magenta) and 6 equiv of F^- (violet) anions.

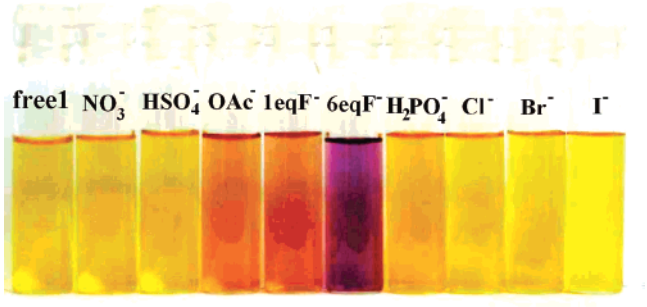

Figure 2. Color changes observed for **1** in MeCN solution (8×10^{-5} M) and the addition of 1 equiv of the corresponding anions as TBA salts and 6 equiv of TBAF.

Table 2. Selected Bond Lengths (Å) and Angles (deg) of **2**[a]

Ru−N(1)	2.046(2)	Ru−N(4)	2.033(2)
Ru−N(2)	2.038(3)	Ru−N(5)	2.079(3)
Ru−N(3)	2.047(2)	Ru−N(7)	2.082(2)
N(5)−C(21)	1.365(4)	N(6)−C(23)	1.322(5)
N(5)−C(23)	1.342(4)	N(6)−C(22)	1.363(4)
C(21)−C(22)	1.361(5)	C(25)−C(26)	1.368(5)
N(7)−C(26)	1.371(4)	N(8)−C(25)	1.385(4)
N(7)−C(24)	1.333(4)	N(8)−C(24)	1.361(3)
C(23)−C(24)	1.439(4)	N(6)···N(8a)	2.791(3)
N(1)−Ru−N(2)	79.2(1)	N(1)−Ru−N(5)	94.6(1)
N(1)−Ru−N(3)	174.3(1)	N(1)−Ru−N(7)	90.4(1)
N(1)−Ru−N(4)	96.6(1)	N(2)−Ru−N(5)	169.0(1)
N(2)−Ru−N(3)	97.5(1)	N(2)−Ru−N(7)	92.6(1)
N(2)−Ru−N(4)	95.3(1)	N(3)−Ru−N(5)	89.4(1)
N(3)−Ru−N(4)	78.9(1)	N(3)−Ru−N(7)	94.4(1)
N(4)−Ru−N(5)	94.5(1)	N(5)−Ru−N(7)	78.2(1)
C(22)−N(6)−C(23)	105.2(3)	C(24)−N(8)−C(25)	105.6(3)
C(21)−N(5)−C(23)	104.6(3)	C(24)−N(7)−C(26)	106.3(3)
N(5)−C(23)−N(6)	113.3(3)	N(7)−C(24)−N(8)	111.7(3)

[a] Symmetry code: a $-x, -y, -2 - z$; b $1/2 - x, -1/2 - y, z$.

(32) (a) Majumdar, P.; Peng, S.-M.; Goswami, S. *J. Chem. Soc., Dalton Trans.* **1998**, 1569. (b) Majumdar, P.; Kamar, K. K.; Castiñeiras, A.; Goswami, S. *Chem. Commun.* **2001**, 1292. (c) Kamar, K. K.; Falvello, L. R.; Fanwick, P. E.; Kim, J.; Goswami, S. *Dalton Trans.* **2004**, 1827.
(33) (a) Fortin, S.; Beauchamp, A. L. *Inorg. Chem.* **2001**, *40*, 105. (b) Ion, L.; Morales, D.; Perez, J.; Riera, L.; Riera, V.; Kowenicki, R. A.; McPartlin, M. *Chem. Commun.* **2006**, 91.
(34) During the preparation of this manuscript, we became aware of the efforts of Ward et al., who observed the hydrogen-bonded assemblies of ruthenium(II)-biimidazole complex cations and cyanometallate anions: Derossi, S.; Adams, H.; Ward, M. D. *Dalton Trans.* **2007**, 33.
(35) Sprintschnik, G.; Sprintschnik, H. W.; Kirsch, P. P.; Whitten, D. G. *J. Am. Chem. Soc.* **1977**, *99*, 4947.
(36) Dose, E. V.; Wilson, L. J. *Inorg. Chem.* **1978**, *17*, 2660.

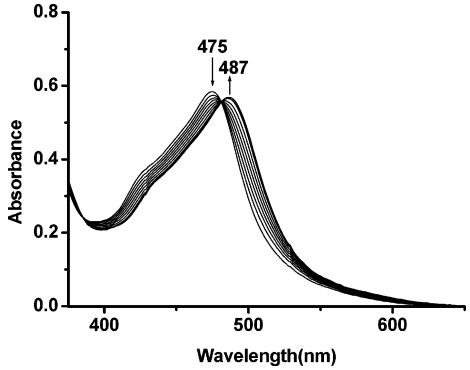

Figure 3. UV−vis titration of **1** in MeCN solution (5×10^{-5} M) upon addition of 1 equiv of $[Bu_4N]H_2PO_4$.

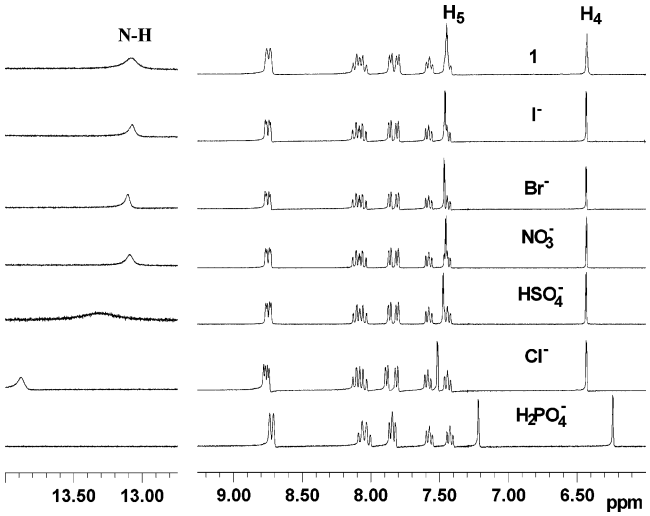

Figure 4. ^{1}H NMR spectra of **1** (7.5×10^{-3} M) in DMSO-d_6 in the absence and presence of 1 equiv of anions.

Synthesis of H_2biim. The H_2biim ligand was synthesized in accordance with the published procedure.[37] Yield: 35%. Anal. Calcd for $C_6H_6N_4$: C, 53.73; H, 4.48; N, 41.79. Found: C, 53.41; H, 4.24; N, 41.56%. FT-IR (cm^{-1}): ν 3143 (m), 3074 (m), 3001 (s), 2896 (s), 2806 (s), 1546 (s), 1436 (m), 1405 (vs), 1333 (s), 1217 (m), 1105 (vs), 939 (s), 888 (m), 763 (m), 748 (s), 690 (m). ^{1}H NMR (DMSO-d_6): δ 7.06 (C−H), 13.34 (N−H).

Syntheses of $Ru(bpy)_2(H_2biim)(PF_6)_2$(1). The title complex was synthesized in accordance with the published procedure.[36] Yield: 81%. ^{1}H NMR (DMSO-d_6): δ 8.75 (d, $J = 2.8$ Hz, 4H, bpy), 8.08 (t, 4H, bpy), 7.84 (d, $J = 5.6$ Hz, 4H, bpy), 7.51 (t, 4H, bpy), 7.46 (d, $J = 1.4$ Hz, 2H, H_2biim-H_5), 6.43 (d, $J = 1.3$ Hz, 2H, H_2biim-H_4), 13.08 (b, 2H, N−H). ESI-MS: m/z 547.1 $[M - 2PF_6 - H]^+$, 274.1 $[M - 2PF_6]^{2+}$.

Synthesis of $[Ru(bpy)_2(Hbiim)]N_3 \cdot H_2O$ (2). NaN_3 (1 mmol, 65 mg) was added to the solution of $[Ru(bpy)_2(H_2biim)]Cl_2$ (**3**) (0.05 mmol, 36 mg) in ethanol (30 mL), and the mixture was stirred at room temperature for 2 h. Then, the solution was filtered, and the filtrate was kept at room temperature to volatilize the solvent. After several days, the deep red crystals of **2** were obtained. Yield: 41.2%. ^{1}H NMR (DMSO-d_6): δ 8.70 (d, $J = 8.1$ Hz, 2H, bpy), 8.02 (t, 1H, bpy), 7.80 (t, 1H, bpy), 7.85 (d, $J = 6.0$ Hz, 1H, bpy), 7.83 (d, $J = 6.1$ Hz, 1H, bpy), 7.55 (t, 1H, bpy), 7.41 (t, 1H, bpy), 7.02 (s, 2H, H_5), 6.06 (s, 2H, H_4).

X-ray Crystallography. Diffraction intensities for **2** were collected at 293 K on a Bruker Smart Apex CCD diffractometer with graphite-monochromated Mo Kα radiation ($\lambda = 0.71073$ Å). Absorption corrections were applied using SADABS.[38] The structures were solved by Patterson methods and refined with the full-matrix least-squares technique using SHELXS-97 and SHELXL-97 programs, respectively.[39,40] Anisotropic thermal parameters were applied to all non-hydrogen atoms. The organic hydrogen atoms were generated geometrically (C−H = 0.96 Å and N−H = 0.86 Å). The hydrogen atoms of the water molecules were located from difference maps and refined with isotropic temperature factors. Analytical expressions of neutral-atom scattering factors were employed, and anomalous dispersion corrections were incorporated. Crystal data and the details of data collection and refinement for **2** are summarized in Table 1. Selected bond distances and bond angles are listed in Table 2.

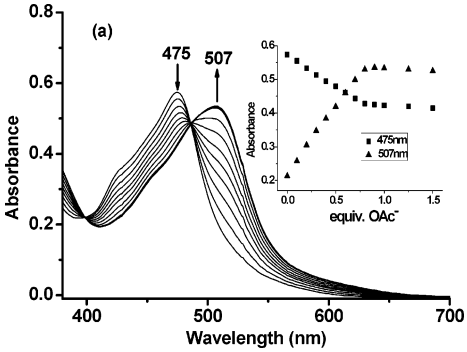

Figure 5. UV−vis titration of **1** in MeCN solution (5×10^{-5} M) upon addition of Bu_4NOAc. Inset: Absorbances at 475 and 507 nm versus equivalents of OAc^- anion.

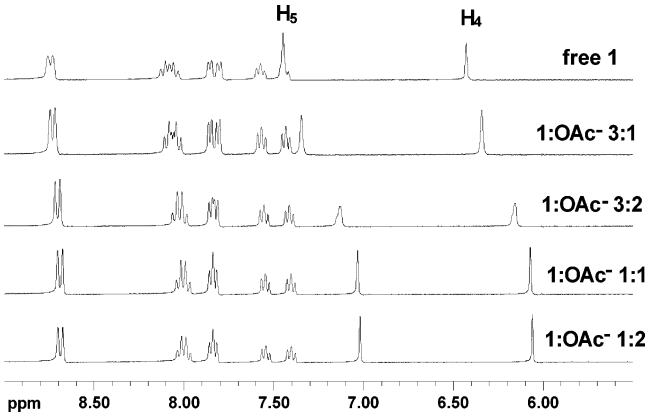

Figure 6. ^{1}H NMR titration of a 7.5×10^{-3} M solution of **1** in DMSO-d_6 with OAc^- anion.

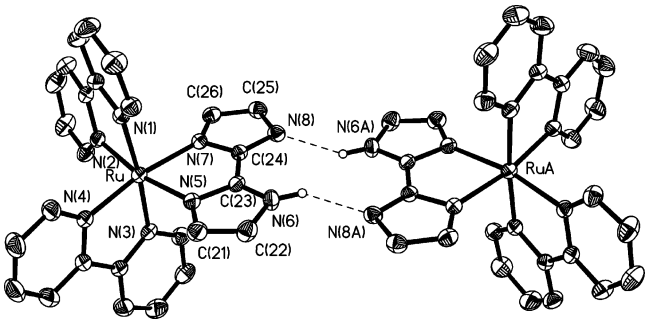

Figure 7. Dimeric structure of **2** linked via hydrogen bonds.

(37) Xiao, J.-C.; Shreeve, J. M. *J. Org. Chem.* **2005**, *70*, 3072.

(38) Blessing, R. H. *Acta. Crystallogr., Sect. A* **1995**, *51*, 33.

(39) Sheldrick, G. M. *SHELXS-97, Program for Crystal Structure Solution*; Göttingen University: Göttingen, Germany, 1997.

(40) Sheldrick, G. M. *SHELXL-97, Program for Crystal Structure Refinement*; Göttingen University: Göttingen, Germany, 1997.

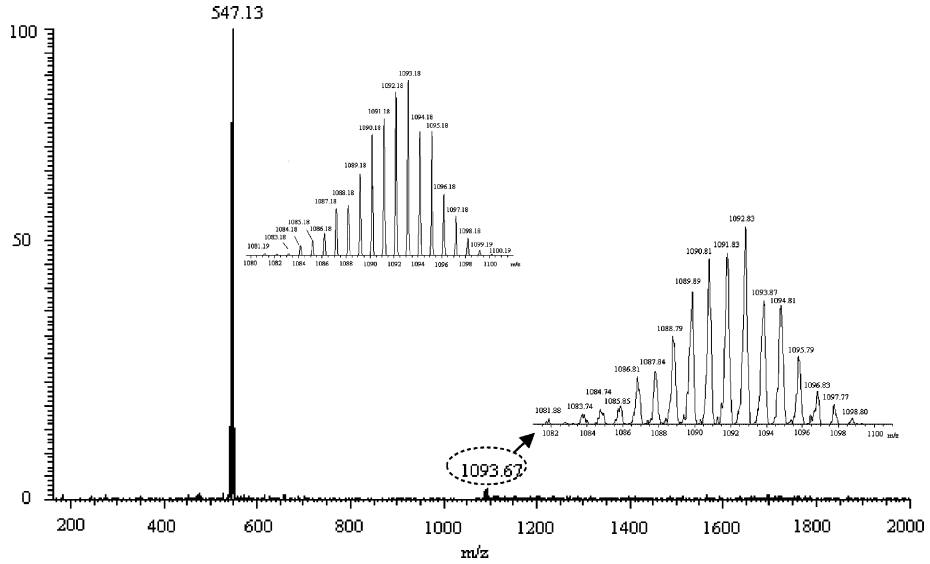

Figure 8. ESI-MS of **2** in MeCN solution. Inset: Amplification of the mass spectrum (bottom) and the calculation for $[\{Ru(bpy)_2(Hbiim)\}_2\text{-}H]^+$ (top).

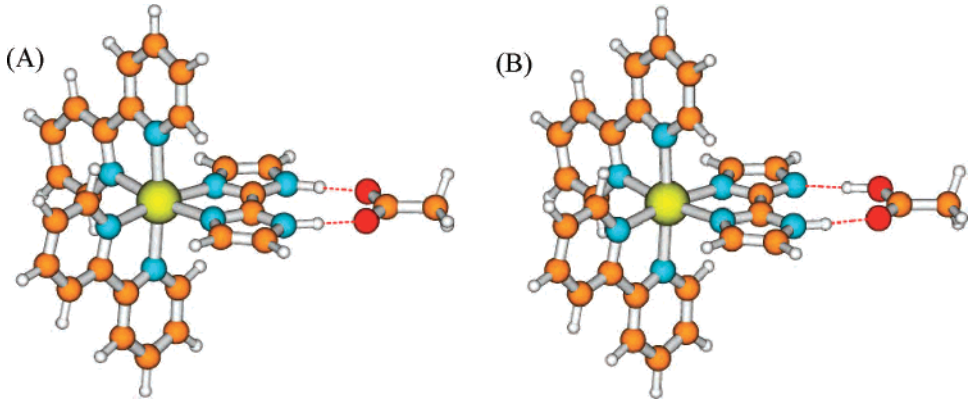

Figure 9. Optimized structures for $\{[Ru(bpy)_2(H_2biim)]\cdot OAc\}$ association using ab initio methods at the level of H-F/LanL2DZ.

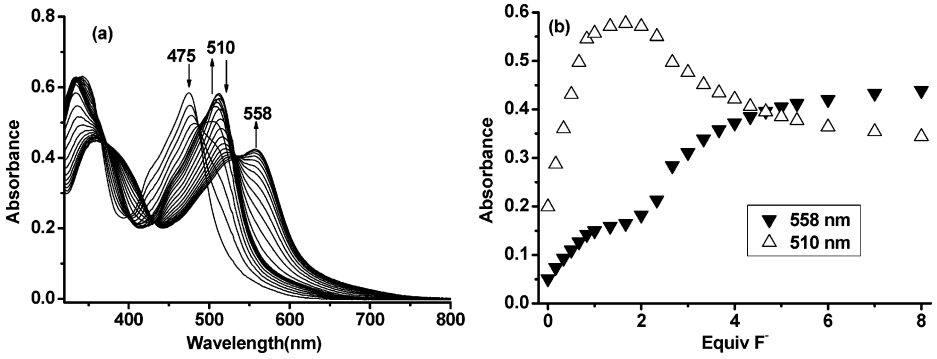

Figure 10. (a) UV−vis titration of **1** in MeCN solution (5×10^{-5} M) upon addition of $[Bu_4N]F$ (0−6 equiv). (b) Absorbances at 510 and 558 nm versus equivalents of F^- anion.

General Spectroscopic Methods. Solvent MeCN used for spectral experiments was distilled from CaH_2 and kept over 4 Å molecular sieves. Tetrabutylammonium (TBA) salts of F^-, Cl^-, Br^-, I^-, NO_3^-, HSO_4^-, $H_2PO_4^-$, and OAc^- were purchased from Alfa Aesar and dissolved in MeCN. Binding constants were performed in duplicate, and the average is reported. All data were manipulated by using the OriginLab software package.

Absorption Spectroscopy. UV−vis spectra were performed on a Shimadzu UV-315 UV−vis spectrophotometer at room temperature. Quartz cuvettes with a 1 cm path length and 3 mL volume were used for all measurements. For a typical titration experiment, 3 μL aliquots of a TBA salt (5×10^{-3} M in MeCN) were added to a 3 mL solution of **1** (5×10^{-5} M in MeCN) by a syringe. For F^- titration, 1 μL aliquots of a Bu_4NF (0.025 M in MeCN) were added to a 3 mL solution of **1** (5×10^{-5} M in MeCN) by a syringe.

Fluorescence Spectroscopy. Emission spectra were measured on a Shimadzu RF-5301PC spectrofluorophotometer at room temperature. Quartz cuvettes with a 1 cm path length and 3 mL volume were used for all fluorescence measurements. For a typical titration experiment, 3 μL aliquots of an TBA salt (5×10^{-3} M in MeCN) were added to a 3 mL solution of **1** (5×10^{-5} M in MeCN) by a syringe. For F^-, 1 μL aliquots of a $[Bu_4N]F$ (0.025 M in MeCN) were added to a 3 mL solution of **1** (5×10^{-5} M in MeCN) by a syringe. The excitation wavelengths were fixed at 470 nm

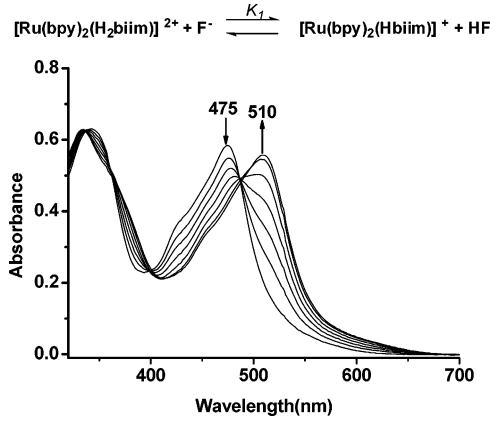

Figure 11. UV−vis titration of **1** in MeCN solution (5×10^{-5} M) upon addition of 0−1 equiv of $[Bu_4N]F$.

with the slit width of 5 nm and repeated at least three times. The luminescence lifetime was measured on an Edinburgh-FLS 920 combined fluorescence lifetime and steady-state spectrometer with the slit width of 1 nm at room temperature. Lifetime was measured in MeCN solution at 5×10^{-5} M at room temperature and fit to a single-exponential decay function.

^{1}H NMR Titration. ^{1}H NMR spectra were recorded on a Varian Mercury-Plus 300 NMR spectrometer with DMSO-d_6 as solvent and TMS as an internal standard. For a typical experiment, 15 μL aliquots of a TBA salt (0.05 M in DMSO-d_6) were added to a DMSO-d_6 solution of **1** (7.5×10^{-3} M). For F^-, 10 μL aliquots of a $[Bu_4N]F$ (0.075 M in DMSO-d_6) were added to a DMSO-d_6 solution of **1** (7.5×10^{-3} M).

Theoretical Calculations. The geometry optimizations were carried out for the isomers **A** and **B** in the gas phase using Hartree−Fock (H−F) ab initio method with the LanL2DZ basis set (effective core potential ECP+DZ for Ru atom, D95 for other atoms);[41] the stable configurations of the complexes were confirmed by the vibrational frequency analysis, in which no imaginary frequency was found for all configurations at the energy minima. To obtain accurate energies for the isomers **A** and **B**, single-point energy calculations for the optimized geometries were further carried out using the density functional theory (DFT)/B3LYP approach and LanL2DZ/6-31+G(d, p) basis set (ECP +DZ for Ru atom and 6-31+G(d, p) for other atoms (C, N, O and H atoms)).[42] All calculations were performed using the Gaussian 03 program package.[43]

Results and Discussion

Interaction with Cl^-, Br^-, I^-, NO_3^-, HSO_4^-, and $H_2PO_4^-$ Anions. Metal-H_2biim complexes have been extensively assembled with anions in the solid state and crystal engineering via hydrogen bonding.[24−29] However, their chemical behavior in solution has seldom been observed.[33,34] To systematically observe the interactions of metalloreceptor for anions, we used the functional complex **1** as a sensor to investigate the interactions with various anions in solution through spectrophotometric titration experiments. When the standard solutions containing the representative anions such as Cl^-, Br^-, I^-, NO_3^-, HSO_4^-, and $H_2PO_4^-$ were added respectively to a 5×10^{-5} M solution of **1** at room temperature, as shown in Figure 1, the original absorption peak at 475 nm, which was assigned to metal−ligand charge transition (MLCT) from Ru(II) to bpy ligand, was unchanged upon addition of Cl^-, Br^-, I^-, NO_3^-, and HSO_4^- anions. However, upon addition of the $H_2PO_4^-$ anion, the band at 475 nm was red-shifted to 487 nm, demonstrating a strong interaction between **1** and the $H_2PO_4^-$ anion. Significantly, the peak was markedly red-shifted to 507 and 558 nm upon addition of the OAc^- and F^- anions, and the original, yellow solution of **1** became orange brown and violet, respectively. Interestingly, these events can be distinguished visually as shown in the picture in Figure 2. The red-shift of the MLCT band can be attributed to the "second-sphere donor−acceptor" interactions between Ru(II)-H_2biim and anions. Such interactions (hydrogen bonding or proton transfer, vide infra) increase the electron density at the metal center and shift the oxidation potential of Ru(II) ion to a less positive value, resulting in the decrease of the MLCT band energy.[44] Obviously, when a stronger interaction takes place (ultimately the H_2biim ligand become a deprotonated anion), more red-shift is observed.

To investigate the binding property of **1** toward $H_2PO_4^-$ anion, titration experiments were carried out as shown in Figure 3. During process of adding 1 equiv of $H_2PO_4^-$ to the solution of **1**, the maximum absorption peak at 475 nm gradually decreases, while a new band at 487 nm forms. The addition of more $H_2PO_4^-$ anion gives rise to precipitation. The appearance of two sharp isosbestic points at 385 and 481 nm in the titration profile indicates that only two species coexist at the equilibrium and form a 1:1 stoichiometry $\{[Ru(bpy)_2(H_2biim)]\cdot H_2PO_4\}$. The binding constant can be determined from the equilibrium as follows:

(41) (a) Hay, P. J.; Wadt, W. R. *J. Chem. Phys.* **1985**, *82*, 270. (b) Wadt, W. R.; Hay, P. J. *J. Chem. Phys.* **1985**, *82*, 284. (c) Hay, P. J.; Wadt, W. R. *J. Chem. Phys.* **1985**, *82*, 299.

(42) (a) Becke, A. D. *J. Chem. Phys.* **1993**, *98*, 5648. (b) Lee, C.; Yang, W.; Parr, R. G. *Phys. Rev. B.* **1988**, *37*, 785. (c) Ditchfield, R.; Hehre, W. J.; Pople, J. A. *J. Chem. Phys.* **1971**, *54*, 724. (d) Hehre, W. J.; Ditchfield, R.; Pople, J. A. *J. Chem. Phys.* **1972**, *56*, 2257. (e) Gordon, M. S. *Chem. Phys. Lett.* **1980**, *76*, 163. (f) Frisch, M. J.; Pople, J. A.; Binkley, J. S. *J. Chem. Phys.* **1984**, *80*, 3265.

(43) Frisch, M. J.; Trucks, G. W.; Schlegel, H. B.; Scuseria, G. E.; Robb, M. A.; Cheeseman, J. R.; Montgomery, J. A., Jr.; Vreven, T.; Kudin, K. N.; Burant, J. C.; Millam, J. M.; Iyengar, S. S.; Tomasi, J.; Barone, V.; Mennucci, B.; Cossi, M.; Scalmani, G.; Rega, N.; Petersson, G. A.; Nakatsuji, H.; Hada, M.; Ehara, M.; Toyota, K.; Fukuda, R.; Hasegawa, J.; Ishida, M.; Nakajima, T.; Honda, Y.; Kitao, O.; Nakai, H.; Klene, M.; Li, X.; Knox, J. E.; Hratchian, H. P.; Cross, J. B.; Bakken, V.; Adamo, C.; Jaramillo, J.; Gomperts, R.; Stratmann, R. E.; Yazyev, O.; Austin, A. J.; Cammi, R.; Pomelli, C.; Ochterski, J. W.; Ayala, P. Y.; Morokuma, K.; Voth, G. A.; Salvador, P.; Dannenberg, J. J.; Zakrzewski, V. G.; Dapprich, S.; Daniels, A. D.; Strain, M. C.; Farkas, O.; Malick, D. K.; Rabuck, A. D.; Raghavachari, K.; Foresman, J. B.; Ortiz, J. V.; Cui, Q.; Baboul, A. G.; Clifford, S.; Cioslowski, J.; Stefanov, B. B.; Liu, G.; Liashenko, A.; Piskorz, P.; Komaromi, I.; Martin, R. L.; Fox, D. J.; Keith, T.; Al-Laham, M. A.; Peng, C. Y.; Nanayakkara, A.; Challacombe, M.; Gill, P. M. W.; Johnson, B.; Chen, W.; Wong, M. W.; Gonzalez, C.; Pople, J. A. *Gaussian 03*, revision D.1; Gaussian, Inc.: Wallingford, CT, 2005.

(44) (a) Balzani, V.; Sabbatini, N.; Scandola, F. *Chem. Rev.* **1986**, *86*, 319. (b) Rampi, M. A.; Indelli, M. T.; Scandola, F.; Pina, F.; Parola, A. J. *Inorg. Chem.* **1996**, *35*, 3355.

$$[Ru(bpy)_2(H_2biim)]^{2+} + H_2PO_4^- \overset{K}{\rightleftharpoons} \{[Ru(bpy)_2(H_2biim)]\cdot H_2PO_4\}$$

$$K = \frac{[Ru(bpy)_2(H_2biim)\cdot H_2PO_4]}{[H_2PO_4^-][Ru(bpy)_2(H_2biim)]} \quad (1)$$

According to the literature,[45] a response function for $H_2PO_4^-$ anion is given by the following mass law:

$$\Delta A = \frac{\Delta\epsilon b\left([S] + [L] + \frac{1}{K}\right) \pm \sqrt{\Delta\epsilon^2 b^2\left([S] + [L] + \frac{1}{K}\right)^2 - 4\Delta\epsilon^2 b^2 [S][L]}}{2} \quad (2)$$

where ΔA refers to the change in absorbance from initial value and [S] and [L] are the concentrations of **1** and $H_2PO_4^-$, respectively. Using the nonlinear curve fitting approach, the binding constant K and the change in molar extinction coefficient $\Delta\epsilon$ were calculated using the data of ΔA observed at each [L]. The best fitting of the experimental data for $H_2PO_4^-$ anion gives log $K = 3.32$.

Hydrogen-bonding interactions between Ru-H_2biim and the above-mentioned anions were also investigated by ^{1}H NMR experiments. As shown in Figure 4, two N−H groups of Ru(II)-H_2biim appeared as a singlet at 13.08 ppm for **1** in DMSO-d_6. The addition of TBA iodide, bromide, nitrate, hydrogensulfate, and chloride shifted this signal to 13.09, 13.10, 13.10 13.45, and 13.88 ppm, respectively. When an equimolar amount of $[Bu_4N]H_2PO_4$ was added to the solution of **1**, the N−H ^{1}H NMR signal finally vanished. Fortunately, the C−H ^{1}H NMR signal of H_5 and H_4 in the imidazole ring displayed markedly upfield shifts of 0.25 and 0.19 ppm, respectively, indicating a strong hydrogen-bonding interaction between **1** and $H_2PO_4^-$ anion.

Interaction with OAc$^-$ Anion. Upon addition of OAc^- to the solution of **1**, the band at 475 nm gradually decreases, while a new peak at 507 nm appears and progressively grows as depicted in Figure 5. The shift of 32 nm in the absorption band is much larger than those observed for Cl^-, Br^-, I^-, NO_3^-, HSO_4^-, and $H_2PO_4^-$, indicating that the interaction of receptor **1** with the OAc^- anion should be stronger. The existence of two isosbestic points at 398 and 486 nm in absorption titration implies that only two species coexist at the equilibrium. The profiles of the absorbance at 475 (decreasing) and 507 nm (increasing) all demonstrate a 1:1 stoichiometry for the receptor−acetate interaction. The equilibrium $[Ru(bpy)_2(H_2biim)]^{2+} + OAc^- \leftrightarrows \{[Ru(bpy)_2(H_2biim)]\cdot OAc\}$ is established, and its binding constant can be given as log $K = 5.44$ via a fitting of the experimental data for the OAc^- anion to eq 2.

A strong interaction between the metalloreceptor **1** and the OAc^- anion was also confirmed by ^{1}H NMR experiment in DMSO-d_6 solution where **1** has a higher solubility. A 7.5×10^{-3} M solution of **1** in DMSO-d_6 was titrated with OAc^- up to 2 equiv. As shown in Figure 6, although the signals of N−H protons in the H_2biim are unobserved in the present case, the chemical shifts of the C−H protons in the H_2biim ligand (H_4 and H_5) are very sensitive to the addition of the OAc^- anion. The chemical shifts of H_4 and H_5 are progressively upfield shifted and remained unchanged upon addition of 1 equiv of OAc^- anion. The final displacements for H_4 and H_5 are 0.37 and 0.45 ppm, respectively. The upfield signal is assigned to H_4 because it is closer to the bpy ligand and suffered from the ring current effect of bpy.[46] The lower-field H_5 signal is more sensitive because it is nearer to the N−H group, which forms the hydrogen-bonding interaction with OAc^-. This is consistent with the observation of the interaction between $[ReCl_2(PPh_3)_2(H_2biim)]^+$ and carboxylates via a variable-temperature ^{1}H NMR experiment[33a] and implies formation of {[[Ru(bpy)$_2$(H_2biim)] OAc} complex via charge-assisted hydrogen bonding.[27a,28a] The formation of the {[Ru(bpy)$_2$(H_2biim)]·OAc} association in solution was further identified by an ESI-MS experiment (see Figure S1).

Scheme 2. Probable Structure of {[Ru(bpy)$_2$(H_2biim)]·OAc} Association

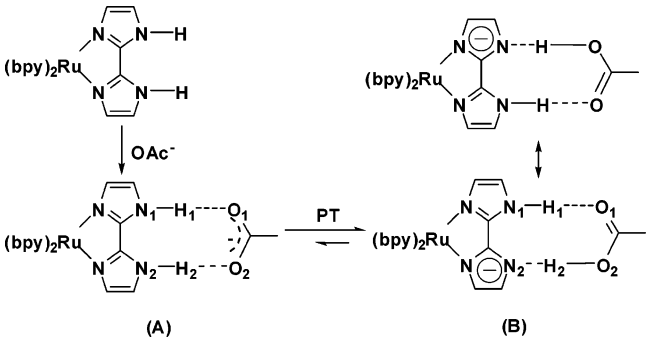

NMR experiments show that **1** interacts with anions via the formation of hydrogen bonding. Why do larger displacements of the chemical shift and absorption band take place upon addition of the OAc^- anion? This can be attributed to the formation of robust hydrogen bonding between **1** and the OAc^- anion because they are geometrically matched and form complementary linear "Y-type" hydrogen bonding.[47] According to one view, "all hydrogen bonding can be considered as incipient proton-transfer reactions, and for strong hydrogen bonding, this reaction can be in a very advanced state".[48] This process should be related to the acidity of N−H group in a given receptor and the basicity of anion. Indeed, Beauchamp and Fortin have successfully proved, via ^{1}H NMR techniques, that there is more upfield displacement of the H_4 and H_5 resonances in a paramagnetic Re(III)-H_2biim complex as the pKa(aq) values of the carboxylic acid is increased.[33a] In the present case, the pK_a of the acetic acid (4.75) is much larger than those of H_3PO_4

(45) (a) Liu, Y.; Han, B.-H.; Chen, Y-T. *J. Phys. Chem. B* **2002**, *106*, 4678.

(46) (a) Hitchcock, P. B.; Seddon, K. R.; Turp, J. E.; Yousif, Y. Z.; Zora, J. A.; Constable, E. C.; Wernberg, O. *J. Chem. Soc., Dalton. Trans.* **1988**, 1837. (b) Ye, B.-H.; Ji, L.-N.; Xue, F.; Mak, T. C. W. *Transition Met. Chem.* **1999**, *24*, 8.

(47) (a) Smith, P. J.; Reddington, M. V.; Wilcox, C. S. *Tetrahedron Lett.* **1992**, *41*, 6085. (b) Fan, E.; van Arman, S. A.; Kincaid, S.; Hamilton, A. D. *J. Am. Chem. Soc.* **1993**, *115*, 369. (c) Boiocchi, M.; Boca, L. D.; Gómez, D. E.; Fabbrizzi, L.; Licchelli, M.; Monzani, E. *J. Am. Chem. Soc.* **2004**, *126*, 16507.

(48) Steiner, T. *Angew. Chem., Int. Ed.* **2002**, *41*, 48.

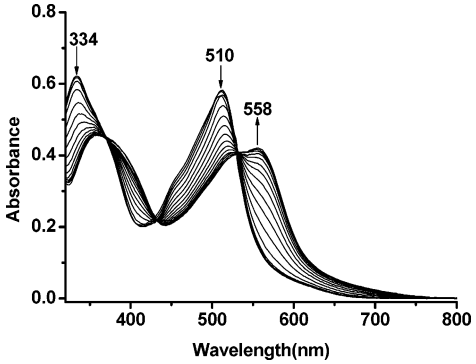

Figure 12. UV−vis titration of **1** in MeCN solution (5×10^{-5} M) upon addition of 2−6 equiv of $[Bu_4N]F$.

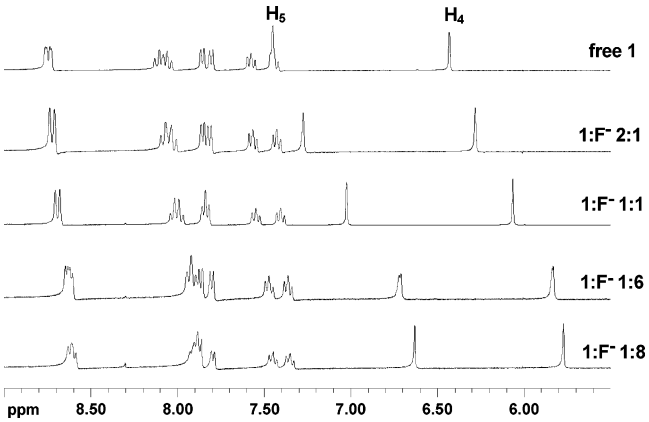

Figure 13. ^{1}H NMR titration of a 7.5×10^{-3} M solution of **1** in DMSO-d_6 with F^- anion.

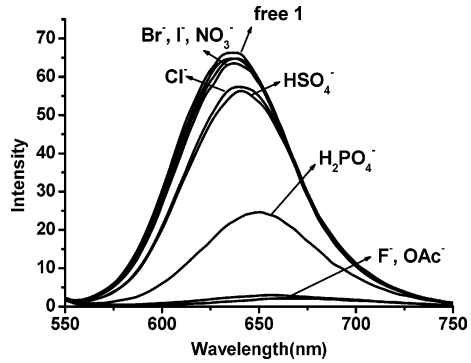

Figure 14. Emission spectra (λ_{ex} = 470 nm) of **1** (5×10^{-5} M) and 1 equiv of anions in MeCN solution.

(pK_{a1} = 1.43) and H_2SO_4 (pK_{a1} = 1.89);[49] thus, the OAc^- anion has a stronger capability of trapping proton from the H_2biim ligand. In this case, the H_2biim ligand is a mono-deprontonated with a strong π-donor ability and much increase of the electronic charge at the Ru(II) center, resulting in a shift of the MLCT band to lower energy.[44] The process is outlined in Scheme 2.

The pK_a(aq) value of acetic acid (4.75)[49] is much lower than the pK_{a1} of sensor **1** (7.2 in MeCN solution).[23b] How can the OAc^- anion trap a proton from **1**? There should be a second factor that assists the proton transfer from **1** to the OAc^- anion. To elucidate this process, NaN_3 with a comparable pK_a (4.62) value[49] but no or weaker hydrogen bonding with the H_2biim ligand was added to the solution of **1**; the color of the solution changed to orange brown upon addition of the OAc^- anion. Their absorption and ^{1}H NMR spectra are almost the same (see Figures S2 and S3). To investigate the structure of the species, we synthesized **2** by reaction of $[Ru(bpy)_2(H_2biim)]Cl_2$ with NaN_3 in EtOH solution, and we measured its structure by X-ray single-crystal determination. As shown in Figure 7, it is a dimeric structure linked via a hydrogen-bonded $R_2^2(10)$ synthon. Although the exact assignment of the hydrogen atom is impossible, the reasonable distribution is that each H_2biim ligand is mono-deprotonated and self-assembles via complementary hydrogen bonding (N(6)···N(8a) = 2.791(3) Å and N(6)−H−N(8a) = 150.2°). The bond lengths and angles of two imidazole rings are almost the same within experimental error. Furthermore, the ESI-MS technique was employed to examine whether such dimeric structure still existed in solution or not. As shown in Figure 8, the ESI-MS spectra give a very clear cluster of isotopic peaks centered at m/z = 1093.7. The mass spectrum of these clusters and the intensity ratio of different isotope peaks are in excellent agreement with the calculated isotope pattern for the expected dimer **2**. In combination with the NMR titration experiments of **1** and OAc^- anion, a similar case may occur in the {$[Ru(bpy)_2(H_2biim)]$·OAc} association. The H_2biim segment and acetate assemble into a heteromeric hydrogen-bonded $R_2^2(9)$ synthon which assists proton transfer from one N−H group of the H_2biim to acetate, forming a complementary hydrogen-bonding association. From the above observations, a conclusion can be drawn out that proton transfer is not only determined by the basicity of anion but also by the strength of hydrogen-bonding interaction.

To further understand the proton transfer in {$[Ru(bpy)_2(H_2biim)]$·OAc}, theoretical calculations were carried out. The optimized geometries show that in the **A** form (Figure 9), the mean torsion angle of O1−O2−N2−N1 is 1.1°, and both O1···H1 and O2···H2 distances are 1.51 Å, indicating a slight deviation from coplanarity and a symmetric interaction between acetate anion and the H_2biim ligand. The acetate group and H_2biim moiety are coplanar (the related torsion angle O1−O2−N2−N1 is 0.4°) in the **B** form, and the distances of O1···H1 and O2···H2 are 1.66 and 1.73 Å, respectively, implying that an asymmetric interaction is presented. The single-point energies at the level of DFT-B3LYP//LanL2DZ/6-31+G(d, p) for the H−F optimized geometries of **A** and **B** are −1764.4471 and −1764.4529 au, respectively, meaning that the total energy of the **B** form is 3.64 kcal/mol lower than that of **A** one. Since **A** and **B** are isomers, their stabilities can be evaluated by comparison of their total energies. The results show that the asymmetric **B** form is more stable than the symmetric **A** one, this is consistent with the experimental observation.

Interaction with F^- Anion. Figure 10 exhibits the complete family of the spectra displacement and absorption intensity variety of the bands at 510 (first increasing and then decreasing) and 558 nm (increasing) during the titration of a 5×10^{-5} M solution of **1** in MeCN with $[Bu_4N]F$. The

(49) *Lange's Handbook of Chemistry*, 15th ed.; Dean, J. A., Ed.; Science Press and McGraw-Hill Education: Beijing, 1999.

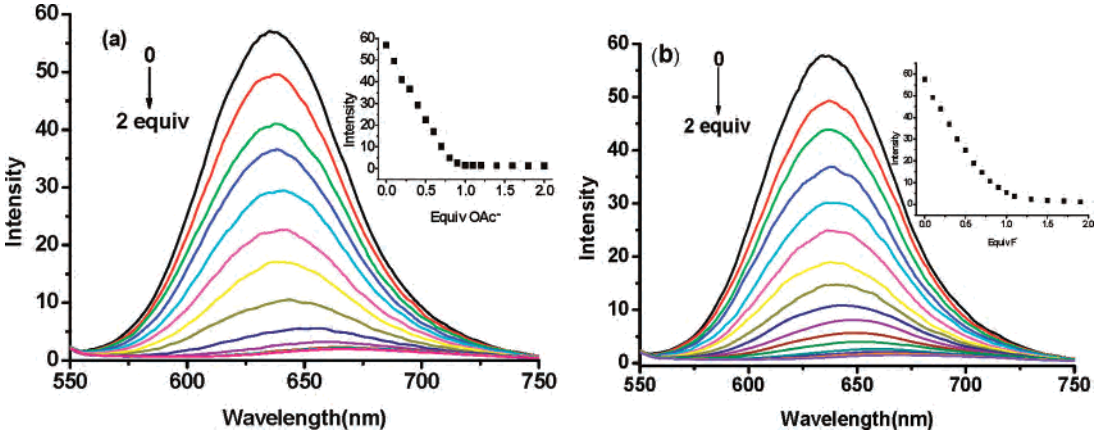

Figure 15. Fluorescent spectra (λ_{em} = 638 nm, λ_{ex} = 470 nm) responses of **1** (5×10^{-5} M) in MeCN solution upon addition of a standard solution of [Bu_4N]OAc (a) and [Bu_4N]F (b) from 0 to 2 equiv. Inset: Intensity at 638 nm versus equiv of anion added.

addition of F^- induces the peak at 475 nm to gradually decrease, and a new absorption band at 510 nm develops while the color changes from yellow to orange brown (see Figure 2), which reaches its limiting value upon addition of 1 equiv of F^-. When 2 equiv of F^- are added to the solution of **1**, the spectral change is negligible. After that, the peak at 510 nm decreases; a new absorption band at 558 nm progressively grows, and the color changes to violet (see Figure 2).

The stepwise changes for the absorption spectra indicate that the interaction may be intricate and involve multistep reactions. From the titration experiment, at least three steps can be distinguished. First, the mono-deprotonation process takes place upon addition of one equiv of F^-, and the solution changes from yellow to orange brown. The new band at 510 nm matches well with the previous observations in the titration experiment by OAc^- and the species **2** (see Figure S2), demonstrating the formation of a mono-deprotonated species. The appearance of three isosbestic points at 363, 399, and 488 nm in the titration profile indicates that only two species coexist at the equilibrium (Figure 11). The profile of the absorbance at 510 nm (increasing) demonstrates a 1:1 stoichiometry for the receptor−F^- interaction. Therefore, this process can be expressed by the following Brönsted acid−base reaction equilibrium:

$$[Ru(bpy)_2(H_2biim)]^{2+} + F^- \overset{K_1}{\rightleftharpoons} [Ru(bpy)_2(Hbiim)]^+ + HF$$

Its binding constant can be given by log K_1 = 5.29 via a fitting of the experimental data of F^- anion to eq 2.

Second, during the addition of 1−2 equiv of F^- to the solution of **1**, the change of absorption spectra is negligible. This can be considered as the formation of the highly stable HF_2^- dimer.[50]

$$HF + F^- \rightleftharpoons HF_2^-$$

On addition of a further excess of [Bu_4N]F to the solution of **1**, the solution changes from orange brown to violet (see Figure 2). The band at 510 nm decreases, and a new band at 558 nm grows. Three isosbestic points at 369, 434, and 532 nm are observed in the titration profile, indicating that only two species coexist at the equilibrium (Figure 12). The new band may pertains to the bi-deprotonated species [$Ru(bpy)_2$(biim)], which forms according to the following equilibrium:

$$[Ru(bpy)_2(Hbiim)]^+ + 2F^- \overset{K_2}{\rightleftharpoons} [Ru(bpy)_2(biim)] + HF_2^-$$

The constant of K_2 is related to the second acidity constant of **1** and to the formation constant of HF_2^-. The titration profile shows that more than two equivalents of F^- is needed to trap the second proton from **1**, forming the bi-deprotonated species [$Ru(bpy)_2$(biim)]. This may be attributed to an especially high pKa_2 value (12) of **1**.[23] On the other hand, the stepwise deprotonation process is fully reversible upon addition of water to the resultant solution, with color turning from violet to orange brown and then to yellow.

A ^1H NMR titration experiment was conducted to further investigate the interaction of **1** with F^- in DMSO-d_6. As shown in Figure 13, upon addition of 0.5 equiv of F^-, the signals of H_4 and H_5 on H_2biim rings shift distinctly upfield because of the charge delocalization on the entire conjugated system with the deprotonation of N−H group. With more equivalents of F^-, these signals further shift upfield, and stop upon addition of 8 equiv of F^- anion. The final displacements for H_4 and H_5 are 0.66 and 0.82 ppm, respectively.

To further confirm the bi-deprotonated species [$Ru(bpy)_2$(biim)], 2 equiv of $NaOCH_3$ was added to a solution of **1**, its absorption and ^1H NMR spectra were performed and compared with the titrated solution of F^- (see Figures S4 and S5). They match well, indicating that the bi-deprotonated species [$Ru(bpy)_2$(biim)] really forms upon addition of 8 equiv of F^- anion.

Fluorescence Properties. The above observations show that the different interactions of **1** with the representative anions: hydrogen bonding and proton transfer, in which one equivalent of strong base such as F^- or OAc^- can remove a N−H proton. Compound **1** emits at 635 nm in MeCN solution at room temperature with a lifetime of 62.79 ± 0.08 ns (see Figure S6), which can be assigned to d−π^* MLCT transition.[23] Therefore, the fluorescence responses to anions

(50) (a) Kang, S. O.; Powell, D.; Day, V. W.; Bowman-James, K. *Angew. Chem., Int. Ed.* **2006**, *45*, 1921. (b) Shenderovich, I. G.; Tolstoy, P. M.; Golubev, N. S.; Smirnov, S. N.; Denisov, G. S.; Limbach, H.-H. *J. Am. Chem. Soc.* **2003**, *125*, 11710.

were employed to observe their interactions. As shown in Figure 14, the changes of fluorescence intensity are negligible upon the addition of Br^-, I^-, and NO_3^- anions because of the weaker interaction between them in solution. These are consistent with those observations in the absorption and NMR experiments. The fluorescence intensities slightly decrease in the cases of Cl^- and HSO_4^-, indicating these anions interact with **1** in solution. As expected, the moderate basicity anion $H_2PO_4^-$ suppresses the fluorescence of **1** and red shifts the emission to 648 nm. The stronger bases and hydrogen binding acceptors such as OAc^- and F^- completely quench the fluorescence of **1**, implying that a N−H proton of H_2biim is trapped by these anions.

To determine the amount of anions required to cause the quenching of **1**, fluorescence titration experiments were carried out with $H_2PO_4^-$, OAc^-, and F^- anions as shown in Figures 15 and S7. When 1 equiv of OAc^- or F^- was added, the emission of **1** was almost completely quenched. This may be attributed to the deprotonation of N−H group in H_2biim.[23a] The mole ratio method for the fluorescent intensity versus equivalents of anion added was applied to examine the stoichiometry of **1** to anion, indicating a 1:1 stoichiometry for the **1**−anion interaction.

Conclusion

In conclusion, we have developed a new anion sensor **1** based on the Ru(II)-bpy moiety as a chromophore and the H_2biim ligand as anion receptor via the formation of hydrogen bonding. The study presents that Ru(II)-H_2bbim is an appropriate receptor for anions via formation of N−H···X hydrogen bonding, mono-proton-transfer system, or deprotonation depending on the interacting anions. These processes are signaled by the change of vivid colors, resulting from the second sphere donor−acceptor interactions between Ru(II)-H_2biim and the anions, and can be distinguished visually. These interactions are not only determined by the basicity of the anion but also by the strength of hydrogen bonding. Fluoride is a particular case because it has a high affinity toward the N−H group, rather than forming hydrogen bonding with the receptor. This may be the result of the formation of a highly stable HF_2^- complex, which allows N−H deprotonation. Therefore, the metal-H_2biim complexes can be stepwise deprotonated and further assembled into a polynuclear cluster bridged by $Hbiim^-$ or $biim^{2-}$ in the presence of an appropriate anion. The design strategy and remarkable photophysical properties of sensor **1** will help to extend the development of anion sensors.

Acknowledgment. The authors thank the reviewers for their kind suggestions. This work was supported by the NSFC (No. 20371052 and 20531070) and NSF of Guangdong (No. 031581 and 06023086).

Supporting Information Available: X-ray crystallographic file in CIF format for the structure determination of **2** and the spectra of the interaction of **1** with anions. This material is available free of charge via the Internet at http://pubs.acs.org.

IC7004562